

# **Surface Phonon Polaritons-Using Perpendicular Electric Fields Monitoring in Mid-infrared Circular Antennas Fabricated by Atomic Layer Deposition Method**

**T. Kawano<sup>1</sup>, Y. Kunichika<sup>1</sup>, J. Miyata<sup>1</sup>, Y. Yamamoto<sup>1</sup>, K. Kasahara<sup>1</sup>,  
N. Ikeda<sup>2</sup>, H. Oosato<sup>2</sup>, and Y. Sugimoto<sup>2</sup>**

*1) College of Science and Engineering, Ritsumeikan University, 1-1-1 Noji-higashi, Kusatsu, Shiga 525-8577, Japan*

*2) National Institute for Materials Science (NIMS), 1-2-1 Sengen, Tsukuba, Ibaraki 305-0047, Japan*

## **Abstract**

Distribution of electric fields normal to the antenna plane in the depth direction was experimentally investigated by using mid-infrared circular antennas that were formed on Al<sub>2</sub>O<sub>3</sub>/SiO<sub>2</sub>/Si and SiO<sub>2</sub>/Al<sub>2</sub>O<sub>3</sub>/Si. The Al<sub>2</sub>O<sub>3</sub> layer was deposited using an atomic layer deposition technique which allowed for layer thickness control with an accuracy of nanometers. The field distribution in the depth direction was estimated by observing the surface phonon polariton signals originating from the SiO<sub>2</sub> layer.

## 1. Introduction

Optical antennas generate optical hotspots, and enhance the local field intensity near the antenna, thereby allowing for efficient photon harvesting. Thus, sufficient absorption is obtainable even from a thin absorption layer, and it is possible that a combination of optical antennas and a thin photo-absorption layer (1) can lead to the achievement of high-performance mid-infrared detectors with high-sensitivity and quick response times. Circular slot antennas are suitable for this purpose because they are polarization independent. When subband transitions are used as photoabsorption-like quantum well infrared photodetectors, an electric field must be created in the growth direction, since subband transitions are only sensitive to electric fields vertical to the substrate surface. Thus, it is important to know the actual field distribution normal to the antenna plane. For electric fields distribution parallel to the antenna plane, so far, we have reported the use of atomic layer deposition (ALD) (2): a thin  $\text{Al}_2\text{O}_3$  layer was deposited on a Si substrate through ALD on which dumbbell-shaped slot antennas were fabricated. ALD was able to grow a layer with its thickness being controlled to an accuracy of  $\sim 1$  nm. By observing the dependence of the Reststrahlen reflection signals arising from  $\text{SiO}_2$  layer, which was naturally formed on the Si substrate, on the  $\text{Al}_2\text{O}_3$  thickness, we could actually gain an understanding of the vertical field localization.

In this study, circular slot antennas were formed on two different substrates (ALD-made  $\text{Al}_2\text{O}_3/\text{SiO}_2/\text{Si}$  and  $\text{SiO}_2/\text{ALD-made } \text{Al}_2\text{O}_3/\text{Si}$ ) in order to know the electric field distribution in the perpendicular direction. The use of an ALD deposited thin  $\text{Al}_2\text{O}_3$  film could make the  $\text{SiO}_2$  layer distant from the circular slot antenna with an accuracy of one nanometer. Surface-Phonon Polariton (SPhP) signals originating from  $\text{SiO}_2$  layer (3) were used to monitor the electric field distribution vertical to the antenna plane by changing the thickness of ALD-made  $\text{Al}_2\text{O}_3$  formed on the  $\text{SiO}_2$ . Unlike Reststrahlen reflection appearing when illuminating electric fields are parallel to the antenna surface, the absorption associated with SPhP emerges only when they are normal to the surface, being used as a monitor of perpendicular electric fields. In the structure where circular antennas were fabricated on  $\text{SiO}_2$  which was on ALD-made  $\text{Al}_2\text{O}_3$ , a difference in vision of SPhP signals occurred, which could be interpreted by taking  $\text{SiO}_2$  bounded by air and  $\text{Al}_2\text{O}_3$ , and having two interfaces into account. Our approach provided versatile information not only on perpendicular electric field distribution in the depth direction but also on SPhP properties.

## 2. Fabrication of circular slot antennas

The shape of a conventional slot antenna is rectangular. In this study, it was modified like a dumbbell so as to increase field-intensity near the feed gap at the center, and to form a single hot spot (3). Another merit of these antennas is that the fabrication is easier than that of dipole antennas, because dipole antennas leave small metal stripes on a substrate. The antenna arrays were fabricated as follows: a thin  $\text{Al}_2\text{O}_3$  was grown using the ALD on a Si substrate. A set of cleaning processes including HF treatment is ordinarily performed to remove an oxide film naturally formed on a Si substrate prior to deposition of dielectric layers. In this study, that process was omitted. Next, Au (40 nm)/Ti (10 nm) were deposited on the substrate. Antenna patterns were made by electron-beam lithography and a lift-off technique followed it, cutting out dumbbell-shaped openings from the metal sheet. One antenna array consisted of 15x5 dumbbell-type slot antennas (DSAs) with each having the same size and dimensions. Besides the antenna arrays, the metal sheet had  $30\ \mu\text{m} \times 30\ \mu\text{m}$  square openings to examine the antenna effect.

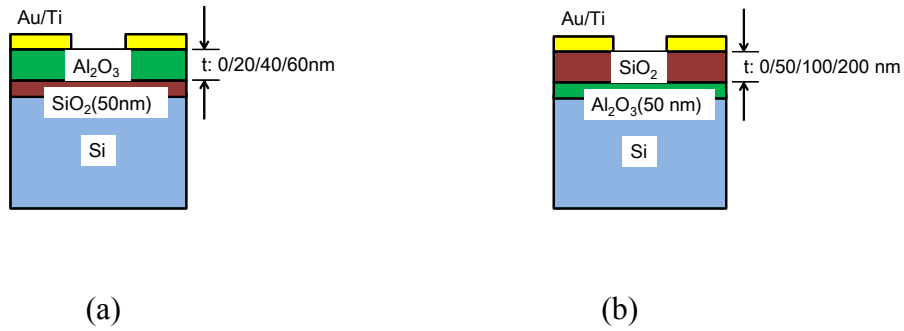


Fig. 1 Cross-sectional view of circular antennas. (a) ALD-made  $\text{Al}_2\text{O}_3/\text{SiO}_2/\text{Si}$  and (b)  $\text{SiO}_2/\text{ALD}$ -made  $\text{Al}_2\text{O}_3/\text{Si}$ . The diameter of circles was varied from 2.8 to 3.6  $\mu\text{m}$ .

## 3. Results and discussions

Figure 2 (a) shows the results for  $R$  of antenna arrays on the  $\text{Al}_2\text{O}_3/\text{SiO}_2/\text{Si}$  substrates. The diameter of antenna  $D$  was 3.6  $\mu\text{m}$ . It was found that a dip appeared around  $1130\ \text{cm}^{-1}$  in the case without an  $\text{Al}_2\text{O}_3$  layer. The dip became weaker as the  $\text{Al}_2\text{O}_3$  layer thickness increased. Reflectivity increase ranging from  $1000\sim 1250\ \text{cm}^{-1}$  was because of the Reststrahlen band of  $\text{SiO}_2$ , in which there was no bulk polariton to transmit radiation, and all incident power was reflected at the interval between the transverse optical phonon frequency and the longitudinal optical phonon frequency. SPhP signals appear at frequencies satisfying the following resonance conditions, when the electromagnetic wave is incident on  $\text{SiO}_2$  from a material having a permittivity  $\varepsilon$ .  $k_{\text{SPhP}}D + \phi = \rho_{\text{mn}}$ , where  $k_{\text{SPhP}}$  is the SPhP wavenumber,

$k_{\text{SPhP}} = k_0 (\epsilon_{\text{SiO}_2} / (\epsilon + \epsilon_{\text{SiO}_2}))^{0.5}$ ,  $k_0$  is the free space wavenumber,  $\phi$  is the phase increment upon the cavity boundary, and  $\rho_{mn}$  is the  $m$ th zero-crossing of the  $n$ th Bessel function (4). Here, SiO<sub>2</sub> and the material are supposed to be semi-infinitely thick. In reality, however, the SiO<sub>2</sub> layer had no such thickness, and it was bounded by Al<sub>2</sub>O<sub>3</sub> (or air when the thickness was 0 nm) on the upper side, and by Si substrate on the lower side, and had two interfaces. It is known that when layer thickness is thin, two SPhP modes appear as a result of resolution of degeneracy. Once degeneracy is resolved, the signal intensities corresponding to two modes should be weak, because the density of states becomes smaller compared with the case of the degenerated state. Since it was troublesome to derive SPhP frequencies in the actual devices, we estimated the SPhP frequencies, for simplicity, by using the above resonance conditions. We also assumed a phase shift of  $-\pi/2$ . It was found that there was no solution which satisfies the resonance condition even for a small  $\rho_{mn}$  such as  $\rho_{01}$  and  $\rho_{11}$  at the lower side in the present circular diameter. SPhP frequencies calculated for air/SiO<sub>2</sub> and Al<sub>2</sub>O<sub>3</sub>/SiO<sub>2</sub> (upper interface) were found to be 1130 cm<sup>-1</sup>, nearly coincident with the observed dip frequency. We performed FDTD calculation, and  $E_z^2$  ( $E_z$ : electric field normal to the antenna surface) dependence in the depth direction could account for the decreasing dip alongside increases in the Al<sub>2</sub>O<sub>3</sub> thickness as shown in Fig. 2 (a).

$R$  for the other structure consisting of circular antennas on SiO<sub>2</sub>/Al<sub>2</sub>O<sub>3</sub>/Si [Fig. 1 (b)] is shown in Fig. 2 (b). In this case, a dip around 1130 cm<sup>-1</sup> was visible when the SiO<sub>2</sub> thickness was 100 nm, and became clearer when the thickness is 200 nm. Comparing the results of 50-nm SiO<sub>2</sub>/Si in Fig. 2 (a) and 50-nm SiO<sub>2</sub>/50-nm Al<sub>2</sub>O<sub>3</sub>/Si in Fig. 2 (b), one will notice that the SPhP signal wasn't apparent in the latter. This was probably because the SiO<sub>2</sub> was bounded by air and Al<sub>2</sub>O<sub>3</sub>, and degeneracy was solved. As mentioned earlier, SPhP frequencies calculated for air/SiO<sub>2</sub> and Al<sub>2</sub>O<sub>3</sub>/SiO<sub>2</sub> were situated at nearly the same frequency (1130 cm<sup>-1</sup>), thereby SPhP signals splitting and disappearing.

The reflectivity became sharply high in the frequency ranges below around 950 cm<sup>-1</sup> when an Al<sub>2</sub>O<sub>3</sub> layer was placed on 50-nm of SiO<sub>2</sub> [Fig. 2 (a)]. Thus, it was apparent that the observed reflection increase was the Reststrahlen reflection of Al<sub>2</sub>O<sub>3</sub> through the electric-field enhancing effects of the antennas. However, one can't see the SPhP signal. According to calculations using the resonance condition, it was concluded that the SPhP signals didn't appear with devices in diameters used in the experiments.

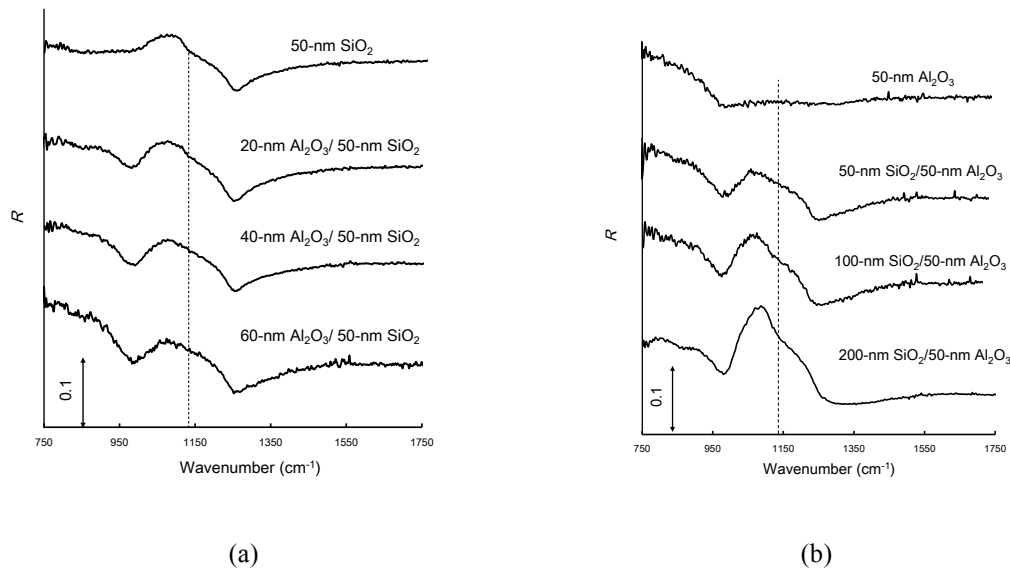


Fig. 2 Normalized reflectivity  $R$  of circular slot antenna array on (a)  $\text{Al}_2\text{O}_3/50\text{-nm SiO}_2/\text{Si}$ , and (b)  $\text{SiO}_2/50\text{-nm Al}_2\text{O}_3/\text{Si}$ . Each array consists of  $10 \times 10$  circular slot antenna elements with a diameter of  $3.6 \mu\text{m}$ . The diameters of circular antennas were all  $3.6 \mu\text{m}$ .

#### 4. Conclusions

Distribution of the electric field vertical to the circular antenna plane in the depth direction was investigated by monitoring the SPhP signals of  $\text{SiO}_2$  films. Our method using ALD provided versatile information not only on the perpendicular electric field distribution in the depth direction, but also fruitful knowledge of SPhP signals in circular slot antennas.

#### References

- (1) W. Wu, A. Bonakdar, and H. Mohseni, *Appl. Phys. Lett.*, **2010**, *96*, 161107.
- (2) Y. Nishimura, S. Mori, T. Kawano, Y. Kunichika, K. Kasahara, T. Yaji, N. Ikeda, H. Oosato, and Y. Sugimoto, in *Proceed. Metamaterials'2014*, **2014**, 53.
- (3) F. Neubrech, D. Weber, D. Enders, T. Nagao, and A. Pucci, *J. Phys. Chem.C*, **2011**, *114*, 7299-7301.
- (4) T. Wang, P. Li, B. Hauer, D.N. Chigrin, and T. Taubner, *Nano Lett.*, **2013**, *13*, 5051.